NASA Technical Memorandum 86884

Preliminary Results of a Study of the Relationship Between Free Stream Turbulence and Stagnation Region Heat Transfer

G. James VanFossen, Jr. and Robert J. Simoneau
Lewis Research Center
Cleveland, Ohio

Prepared for the
Thirtieth International Gas Turbine Conference and Exhibit
sponsored by the American Society of Mechanical Engineers
Houston, Texas, March 17-21, 1985

NASA

PRELIMINARY RESULTS OF A STUDY OF THE RELATIONSHIP BETWEEN FREE STREAM TURBULENCE AND STAGNATION REGION HEAT TRANSFER

G. James VanFossen, Jr. and Robert J. Simoneau
National Aeronautics and Space Administration
Lewis Research Center
Cleveland, Ohio 44135

E-2346

ABSTRACT

A study is being conducted at the NASA Lewis Research Center to investigate the mechanism that causes free stream turbulence to increase heat transfer in the stagnation region of turbine vanes and blades. The work is being conducted in a wind tunnel at atmospheric conditions to facilitate measurements of turbulence and heat transfer. The model size is scaled up to simulate Reynolds numbers (based on leading edge diameter) that are to be expected on a turbine blade leading edge. Reynolds numbers from 13 000 to 177 000 were run in the present tests.

Spanwise averaged heat transfer measurements with high and low turbulence have been made with "rough" and smooth surface stagnation regions. Results of these measurements show that the boundary layer remains laminar in character even in the presence of free stream turbulence at the Reynolds numbers tested. If roughness is added the boundary layer becomes transitional as evidenced by the heat transfer increase with increasing distance from the stagnation line.

Hot wire measurements near the stagnation region downstream of an array of parallel wires has shown that vorticity in the form of mean velocity gradients is amplified as flow approaches the stagnation region. Circumferential traverses of a hot wire probe very near the surface of the cylinder have shown the fluctuating component of velocity changes in character depending on free stream turbulence and Reynolds number.

Finally smoke wire flow visualization and liquid crystal surface heat transfer visualization have been combined to show that, in the wake of an array of parallel wires, heat transfer is a minimum in the wire wakes where the fluctuating component of velocity (local turbulence) was the highest. Heat transfer was found to be the highest between pairs of vortices where the induced velocity is toward the cylinder surface.

NOMENCLATURE

D cylinder diameter, cm

d rod diameter, cm

e height of roughness element, cm

h heat transfer coefficient, $W/m^2 \cdot {}^\circ C$

q" heat flux, W/m^2

Re Reynolds number

T temperature, K

X distance measured upstream from forward stagnation line, cm

z spanwise coordinate, cm

θ circumferential coordinate, deg

INTRODUCTION

In gas turbine blade design, prediction of stagnation region heat transfer is critical because heat flux is usually highest in this region. The heat transfer in the stagnation region can be predicted if the free stream flow is laminar (1). In the gas turbine, flows are highly turbulent with intensities in the range of 8 to 15 percent. If the turbulence intensity in the free stream is higher than say 1 percent, heat transfer in the stagnation region is augmented.

Flow in the stagnation region of a turbine blade can be simulated by a cylinder in crossflow. There have been many experimental investigations of the effect of turbulence intensity on heat transfer to a cylinder in crossflow some of which are given in Refs. 2 to 6. The bulk of these investigations have measured an increase in heat transfer in the stagnation region for some increased level of free stream turbulence and then tried to correlate the heat transfer increase to some parameter involving the turbulence intensity. This approach has had limited success. Trends are clearly present but there is great scatter in the data; particularly between the data of different researchers.

The mathematical modeling of stagnation region flow has been divided into several areas. One set of modelers has attempted to utilize the two dimensional boundary layer equations and develop a turbulence model

that can predict the level of heat transfer (2,7,8). The results are a correlation of the mixing length or turbulent viscosity and Prandtl number with other flow parameters.

A more plausible model of heat transfer augmentation by free stream turbulence is the vortex stretching model. It is hypothesized that, as vortical filaments with components of their axes normal to the stagnation line and normal to the free stream flow are convected into the stagnation region, they are stretched and tilted due to the divergence of streamlines and acceleration around the body. Through conservation of angular momentum, this stretching causes the vorticity to be intensified. This increased vorticity is hypothesized to be the cause of the augmented heat transfer in the stagnation region. Some examples of the work on this theory are given in Refs. 9 to 14 and a review of the work is given in Ref. 15. In Refs. 9 and 10 it was deduced that the mathmatical model allowed only turbulent eddies above a certain neutral scale to enter the Hiemenz flow, Ref. 16, boundary layer. Once inside the boundary layer, however, they could be broken down into smaller scale eddies by the action of viscosity. The three-dimensional vorticity transport equations were solved for a free stream velocity that was periodic in the spanwise coordinate. This boundary condition supplied the vorticity to the stagnation region in an orientation which allowed it to be stretched by the mean flow. A few special cases where the period in velocity was near the neutral scale have been solved. It was found that the thermal boundary layer was much more sensitive to external vorticity than the hydrodynamic boundary layer.

In Ref. 11 measurements of grid turbulence that contained eddies of all orientations near the stagnation point of a circular cylinder showed that eddies with scales much larger than the cylinder diameter are not amplified as they approach the stagnation point. Small scale eddies, however, were found to be amplified as they approached the cylinder. The measurements of Ref. 11 were external to the boundary layer. In Refs. 12 and 13 a hotwire was used to measure the amplification of turbulence near the stagnation point of both a cylinder and an airfoil. The turbulence was produced by an upstream array of parallel rods. Spectral measurements were then used to deduce a so called most amplified scale. Flow visualization with smoke also showed a regular array of vortex pairs near the stagnation point, the array of vortex pairs was clearly outside the theoretical laminar boundary layer.

In Ref. 14 vortex formation near the stagnation region of a bluff body from the wakes of an array of parallel wires placed upstream was studied. It was determined that there was a threshold for vortex formation. If the wires were too far upstream or the Reynolds number was too small, no vortices were formed on the bluff body. Heat transfer augmentation in the stagnation region was found to increase sharply when vortices were formed. The size of the vortices was found to scale with the width of the upstream disturbance wake and not with boundary layer thickness.

Calculations and measurements made in Ref. 5 concluded that the boundary layer velocity profiles are essentially laminar even in the presence of free stream turbulence. The temperature field, however, was found more sensitive to free stream turbulence. This implies that heat transfer will be increased more than skin friction by free stream turbulence.

In this paper a collection of experimental observations will be assembled in order to construct a picture of this complex phenomenon. Spanwise average heat transfer data will be presented to show the effect of free stream turbulence and surface roughness on the condition (laminar or turbulent) of the thermal boundary layer. Hot wire measurements will be used to show how vorticity from mean velocity gradients is amplified as it approaches the stagnation region. Finally, a combination of flow visualization using the smoke wire technique and thermal visualization using liquid crystals will be used to show the relationship between vortex pairs produced by mean velocity gradients and the spanwise heat transfer distribution.

APPARATUS

Wind Tunnel

All tests were conducted in the wind tunnel shown schematically in Fig. 1. Room air first flowed through a turbulence damping screen with an 18x18 mesh of 0.24 mm (0.0095 in) diameter wire. Large scale turbulence from the room was then broken up by flowing through a honeycomb of approximately 12 000 plastic soda straws which were 0.64 cm (0.25 in) in diameter by 19.69 cm (7.75 in) long. The air then passed through a final damping screen identical to the first. A 4.85:1 contraction (contraction in spanwise direction only) then accelerated the air entering the test section. The maximum velocity attainable in the test section was about 46 m/sec (150 ft/sec) and the clear tunnel turbulence level was less than 0.5 percent at all flow rates.

The test section was 15.2 cm (6.0 in) wide by 68.6 cm (27.0 in) high. The models were mounted horizontally in the tunnel. Hot wire surveys and smoke wire flow visualization indicated that the center 7.6 cm (3.0 in) of the tunnel was free from turbulence generated by the sidewall boundary layer. All measurements were confined to this center region of the tunnel test section.

After leaving the test section, the flow passed through a transition section into a 10 in pipe, through two long radius elbows, a flow straightener and into an orifice run. The orifice plate had a diameter of 19.1 cm (7.5 in). The flow rates used in these tests were measured with this orifice. Air then passed through a 10 in butterfly valve which was used to control the flow rate and then to the building altitude exhaust system.

The temperature of the air entering the wind tunnel was measured by four exposed ball Chromel-Alumel thermocouples around the perimeter of the inlet. These four temperatures were averaged to give the total or stagnation temperature.

Turbulence Generators

For some of the high turbulence cases, a turbulence generating biplane grid of 0.318 cm (0.125 in) rods spaced 10 rod diameters apart was installed 79.6 rod diameters upstream of the model leading edge. For the flow visualization tests and some of the heat transfer tests an array of parallel 0.051 cm (0.020 in) wires spaced 12.5 wire diameters apart were installed 547.5 wire diameters (4.21 cylinder diameters) upstream of the model leading edge. For the spanwise hot wire traverses, the same parallel wire array was used but the wires were spaced 37.5 wire diameters apart.

Hot Wire

Turbulence measurements were made with a constant temperature hot wire anemometer. Signals were linearized and the mean component of velocity was read on an integrating digital voltmeter with an adjustable time constant. The fluctuating component was read on a true RMS voltmeter which also had an adjustable time constant. The hot wire probe was a 4×10^{-6} meter diameter,

tungsten, single wire probe. The hot wire was calibrated before each use in a free jet of air at nearly the same temperature (±1 °C) as the wind tunnel flow. The hot wire system frequency response was determined to be around 30 kHz by the standard square wave test.

Turbulence scale was estimated using an autocorrelation of the hot wire signal. The autocorrelation was obtained on a dual channel fast Fourier transform (FFT) spectrum analyzer. The area under the autocorrelation function gave an integral time scale. This time scale was then multiplied by the mean velocity to obtain a measure of the integral length scale.

Smoke Wire

Flow visualization was accomplished using the smoke wire technique described in Ref. 17. A 0.008 cm (0.003 in) wire was stretched across the tunnel parallel to the cylinder axis slightly below the stagnation plane. The wire was coated with oil as recommended in Ref. 17 using a cotton swab. A timing circuit was then used to start current flow to heat the wire and vaporize the oil and, after an adjustable delay, fire a strobe light to expose the film. A 4 by 5 graphic camera with a polaroid back was used initially to determine if all parameters were set correctly and that everything was working properly. A 35 mm camera with telephoto lens and closeup attachments was then used to make high quality images of the flow and heat transfer patterns in the stagnation region. Two strobe lights were used, one from each side of the tunnel. It was found that the best lighting angle for smoke visualization was at 90° from the viewing angle. This angle was not an optimum angle for the viewing of the liquid crystal models. As explained in Ref. 18 if the lighting angle and the viewing angle are not the same, there is a shift in color of the liquid crystal. Thus the simultaneous smoke and liquid crystal thermal visualization photographs can only be used to obtain qualitative heat transfer results.

TEST SPECIMENS

Spanwise Averaged Heat Transfer

Spanwise averaged heat transfer coefficients were measured on a 6.6 cm (2.6 in) diameter cylinder. The cylinder was 15.2 cm (6 in) long and was made of wood. Figure 2 is a photograph of this model. Heat transfer coefficients around the circumference of the cylinder were measured using electrically heated copper strips. Each strip was 6.6 cm (2.6 in) long by 0.51 cm (0.21 in) wide and 0.318 cm (0.125 in) deep. A typical copper heat flux gage is shown in Fig. 3. A Kapton encapsulated electric heater was fastened to the back of each copper strip with pressure sensitive adhesive. A stainless steel sheathed, closed, grounded ball, Chromel-Alumel thermocouple was soft soldered into a groove in each copper strip. The copper heat flux gages were embedded in the surface of the cylinder at 10° intervals around the circumference. The average gap between copper strips was 0.10 cm (0.04 in) and was filled with epoxy. There were eight copper strips but only the inner six strips were used as measuring gages; the outer two served as guard heaters to minimize heat loss by conduction. Guard heaters were also used on the ends of the copper strip gages as shown on Fig. 2. A guard heater was also used behind the measuring gages to stop radial heat conduction to the rear of the cylinder. A thin coat of lacquer was sprayed on the surface of the cylinder and the copper gages to keep the copper from oxidizing and changing emissivity. In operation the copper strips were maintained at a constant temperature by a controller described in Ref. 19. The data reduction technique used for the spanwise average model is also described in Ref. 19.

For some of the tests with the spanwise average heat transfer model it was desired to investigate the effect of surface roughness. This was accomplished by spraying a coat of clear lacquer onto the model, sand was then sprinkled on the wet surface from an ordinary salt shaker. Another thin coat of lacquer then held the sand in place. A profilometer was used to try and measure the roughness but the roughness elements were too large for this instrument. An optical comparator was used to obtain an estimate of the roughness. The maximum height of any one roughness element was found to be 0.0572 cm (0.0225 in). The average height of the roughness elements above the surface was 0.033 cm (0.013 in) which gave a relative roughness, e/D = 0.005.

An afterbody was used with the cylinder for some tests to eliminate the alternate vortex shedding from the rear of the cylinder. The afterbody consisted of a 5.08 cm (2.0 in) straight segment which was tangent to the cylinder surface 90° from the stagnation line. A 10° wedge then extended downstream and ended in a cylindrical trailing edge 0.3175 cm (0.125 in) in diameter.

Liquid Crystal Models

Spanwise variations in heat transfer coefficient were mapped using three different models which are shown in Fig. 4. One of the models is a cylinder with the same dimensions as the spanwise average heat transfer model. Another model had the same dimensions as the spanwise average model plus the afterbody and the third model was scaled to one-half the size of the spanwise average plus afterbody.

All the liquid crystal models were constructed using the techniques in Ref. 18. Briefly, a heater element consisting of polyester sheet with a vapor deposited gold layer was fastened to the model surface with double sided tape. Buss bars of copper foil were fastened to the heater edges parallel to the cylinder axis located at the rear of the cylinder. Silver conductive paint was used to improve electrical conductance between the copper foil and the gold. A commercially available plastic sheet which contained cholesteric liquid crystals was fastened over the heater with double sided tape.

The gold heater was checked for uniformity in still air using the liquid crystal sheets to monitor temperature gradients. The liquid crystal was calibrated in a water bath so the temperature of the yellow color was known. The yellow color was found to indicate a temperature of 54.8 ± 0.2 °C (130.6 ± 0.4 °F).

In operation, the cylinder was heated by passing an electric current through the gold film. This supplied a uniform heat flux at the surface of the cylinder. Electric power to the model was adjusted so that the area of interests on the surface turned a yellow color. Neglecting radiation and conduction losses which are small, the heat transfer coefficient can be computed as:

$$h = \frac{q''}{(T_{yellow} - T_{air})}$$

Thus the yellow color traces an iso-heat transfer coefficient contour on the model.

Traversing Cylinder

Turbulence measurements near the surface of the cylinder were made using the cylinder shown in Fig. 5. This cylinder was made of wood and had a hole drilled through the cylinder along a diameter. A hot wire

probe could be inserted through this hole and positioned very close to the surface. The area around the hot wire prongs was filled in with modeling clay to match the contour of the cylinder. The hot wire cylinder extended through holes in the tunnel walls; felt was used as a seal between the cylinder and the walls. The cylinder could thus be traversed axially across the tunnel span or rotated about its axis carrying the hot wire with it.

ERROR ANALYSIS

An error analysis was performed for each of the spanwise average heat transfer data points by the method of Kline and McClintock (Ref. 20). The average error for all the data points was found to be 5.7 percent and the maximum error for any one data point was 7.8 percent. Error estimates of the hot wire and liquid crystal data were not made.

RESULTS AND DISCUSSION

In this section, spanwise average heat transfer distributions around a circular cylinder in cross flow will be presented for high and low free stream turbulence. The effect of surface roughness will also be presented for both high and low free stream turbulence. Hot wire measurements will be presented to demonstrate amplification of vorticity in the free stream as the flow approaches the stagnation region. Finally, flow visualization and thermal visualization will be combined to show the relationship between vortex pairs formed in the stagnation region and spanwise variations in surface heat transfer.

Spanwise Averaged Heat Transfer

Figure 6 shows Nusselt number as a function of angle from the stagnation point for the four cases mentioned above. All the data on Fig. 6 were taken at a Reynolds number based on free stream conditions and cylinder diameter of 177 000. Low turbulence data were taken with clear tunnel and high turbulence data were taken with a biplane grid. The grid produced turbulence of about 2.4 percent with a scale of 0.50 cm (0.20 in). Also plotted on the figure is an exact solution of the laminar boundary layer equations due to Ref. 1. The data shown on Fig. 6 were for the cylinder without the afterbody; data taken with the afterbody in place were found to be identical within experimental error.

Smooth Surface - Low Turbulence. The agreement between the exact solution and the smooth cylinder, low turbulence data is well within the experimental error and thus confirms the accuracy of the experimental method.

Smooth Surface - High Turbulence. The Nusselt number distribution around the cylinder placed downstream of the biplane grid is also shown on Fig. 6. The effect of turbulence is to increase the heat transfer virtually uniformly around the circumference (measurements were only made up to 50° from stagnation) by about 30 percent. This agrees well with the data of other observers; for example the theory of Ref. 2 predicts an increase in Nusselt number at the stagnation point of 27.8 percent for these conditions.

Rough Surface - Low Turbulence. As seen on Fig. 6, the addition of sand roughness to cylinder surface does not change the heat transfer rate at the stagnation point from the smooth surface case. As the angle from stagnation increases, however, the heat transfer rate also increases. This is most likely due to boundary layer transition triggered by the roughness elements.

Rough Surface - High Turbulence. The final set of symbols on Fig. 6 is for the sand roughened surface with 2.4 percent free stream turbulence. The effect of free stream turbulence is seen to be greater nearest the stagnation point where the heat transfer rate is again increased by about 30 percent over the low turbulence case. As the angle from stagnation becomes larger, the high and low turbulence data (rough surface) merge as the boundary layer becomes more turbulent.

Surface roughness has no effect on heat transfer at the stagnation line but changes the character of the boundary layer in the downstream direction. This indicates that the boundary layer on the smooth surface must remain laminar in character at the Reynolds numbers tested, i.e. there is no turbulence produced within the boundary layer. Free stream turbulence must somehow act on a laminar boundary layer to augment heat transfer.

Hot Wire Measurements

Streamwise traverse. Figure 7 shows the results of a streamwise traverse of a single hot wire with the wire oriented parallel to the 6.6 cm (2.6 in) diameter cylinder axis and as close as possible to the plane of the stagnation streamline. An array of 0.05 cm (0.02 in) parallel wires spaced 12.5 wire diameters apart was located 4.21 cylinder diameters (547.5 wire diameters) upstream of the stagnation point. This wire array produces vorticity (gradients in the mean velocity) in an orientation that can be stretched and amplified. The traverse was made from 0.044 to 3.06 cylinder diameters upstream of the stagnation point. Shown on the figure are both the mean velocity and the root mean square of the fluctuating component of velocity.

The traverse shown was made at a Reynolds number based on cylinder diameter of 177 000 and is typical of all traverses made over the Reynolds number range (31 000 to 177 000). The mean velocity is seen to fall monotonically as the stagnation region is approached. The fluctuating velocity, however, first decays as we move downstream from the grid (from right to left on Fig. 7) and then sharply increases and peaks at about 0.085 cylinder diameters upstream from the stagnation point. This peak is far outside the predicted laminar boundary layer thickness of 0.003 cylinder diameters (Ref. 16). These results are very similar to those of (Ref. 12).

Spanwise traverse. Two spanwise traverses of a hot wire oriented perpendicular to the cylinder axis and centered in the plane of the stagnation streamline are shown on Fig. 8. The cylinder leading edge was located 4.21 cylinder diameters downstream of an array of 0.05 cm (0.02 in) parallel wires which were spaced 37.5 wire diameters apart. Both traverses were made at a Reynolds number based on cylinder diameter of 31 000 and are typical of those for the complete Reynolds number range. Both traverses are presented at the same scale in Fig. 8. For the traverse taken at 1.06 cylinder diameters upstream from the stagnation line one can clearly see the wire wakes in the mean velocity trace. The turbulent fluctuations are seen to be high in the wire wakes and low in the realtively undisturbed flow between wires. At 0.0095 cylinder diameters upstream, the level of the mean velocity is greatly decreased. The

depth of the wake is seen to be increased which indicates an increase in vorticity as the stagnation region is approached. The fluctuating component of velocity is also seen to increase in the wire wakes as the stagnation region is approached.

Circumferential traverses. A hot wire oriented parallel to the cylinder axis and located 0.012 cylinder diameters from the cylinder surface was traversed in the circumferential direction ±21° at a Reynolds number based on cylinder diameter of 125 000. Figure 9(a) shows the traverse made for the clear tunnel case, i.e. free stream turbulence intensity less than 0.5 percent. The mean velocity is seen to increase with angle as the flow accelerates around the body. The fluctuating component of velocity has a minimum at the stagnation point. This functional form of the fluctuating velocity with angle is independent of Reynolds number for all flows tested with the clear tunnel. Figure 9(b) shows the same quantities but with an array of parallel 0.05 cm (0.02 in) wires spaced 12.5 wire diameters apart located 547.5 wire diameters upstream of the stagnation line. The mean velocity trace is identical to that for the clear tunnel. However, the fluctuating velocity has completely changed. The minimum at the stagnation line seen in the clear tunnel case has changed to a maximum and the level away from the stagnation region is decreased. The large variations in fluctuating velocity with angle seen in the clear tunnel case have been damped. This change in character is Reynold number dependent; below a Reynolds number of 95 000 based on cylinder diameter (730 based on wire diameter), the fluctuating velocity has a minimum with or without a wire array as seen in Fig. 9(a). Above a Reynolds number of 95 000 the fluctuating velocity looks like Fig. 9(b). We have no explanation for this phenomenon.

Simultaneous Flow - Thermal Visualization

The smoke wire flow visualization technique was combined with the liquid crystal thermal visualization technique to show the relationship between spanwise variations in heat transfer and vortices in the stagnation region. These vortices were formed from the wakes of wires upstream of the cylindrical leading edge arranged as shown in Fig. 5. Figure 10 is a photograph of the leading edge region for the 6.6 cm (2.6 in) diameter cylindrical leading edge model with afterbody taken at a Reynolds number of 13 000. Note that the Reynolds number for the wires is about 100; for wire Reynolds numbers less than 120, the wakes are laminar, i.e., no Karman trails are formed. The dark lines on the surface of the model were drawn in a 1.27 cm (0.5 in) square grid pattern for visual scaling. Figure 11 is a sketch of the model and relative camera position.

The smoke shows that a vortex pair is formed from the wake of each wire. The vortices are well outside the theoretical laminar boundary layer. The dark, vertical stripes in the liquid crystal are regions of low temperature and thus high heat transfer. Thus, contrary to expectations, the picture shows that the regions of high heat transfer are not under the vortices but between vortex pairs where the free stream turbulence was seen to be a minimum. In this region the induced velocity from neighboring vortex pairs is directed toward the cylinder surface. Conversly, the region of minimum heat transfer is seen to be directly under the vortex pair. This was the region of highest free stream turbulence as measured by a hot wire outside the boundary layer. Figure 12 shows schematically the spatial relationship of the wires, wakes, vortex pairs and the peaks in heat transfer.

The heat transfer-vortex pattern was observed to be the same for all three models shown in Fig. 4. For the cylinder without the afterbody the heat transfer-vortex pattern remained unchanged relative to the model with the afterbody. The half size model with afterbody had the same heat transfer pattern but the vortices appeared smaller in diameter at the same free stream velocity. The spanwise spacing of vortex pairs remained equal to the wire spacing. The Reynolds number for the half scale model was one-half that for the large cylinder with afterbody.

The spanwise heat transfer coefficient variation along the stagnation line, (i.e, maximum h - minimum h)/0.5 (maximum h + minimum h) was found to vary from 7 percent at a Reynolds number of 16 000 to 16 percent at a Reynolds number of 89 000 for the half scale model. This is the same magnitude found in Ref. 21 for spanwise variations in mass transfer caused by periodic irregularities in a screen. Similar measurements were not made for the other models.

High speed motion pictures of smoke near the stagnation point of the cylinder without afterbody were taken at a Reynolds number of 13 000. They showed that vortices still were formed in the stagnation region but the stagnation point oscillated back and forth due to alternate vortex shedding from the rear of the cylinder.

Vortices were only visible for Reynolds numbers based on wire diameter of less than about 120. At higher Reynolds numbers the wire wakes became unstable and finally fully turbulent making it impossible to see the vortices. The heat transfer pattern, however, remained unchanged at all Reynolds numbers indicating that the vortices must still be there but could not be seen. A time exposure photograph was taken hoping that the random fluctuations from the wire wakes would be averaged out and the relatively steady vortex pattern could thus be made visible. The random fluctuations were indeed averaged out but no steady vortices could be seen.

SUMMARY OF RESULTS

In this report, preliminary results of a study to investigate the relationship between free stream turbulence and heat transfer augmentation in the stagnation region were presented. The effect of free stream turbulence and surface roughness on spanwise averaged heat transfer was investigated. Turbulence measurements were made upstream of a cylinder placed in the wake of an array of parallel wires that were perpendicular to the cylinder axis. Finally, flow visualization and thermal visualization techniques were combined to show the relationship between vortices in the stagnation region and spanwise variations in heat transfer.

The major conclusions were:

1. Surface roughness has no effect on heat transfer at the stagnation point.
2. Free stream turbulence has the same effect on heat transfer at the stagnation point for smooth and rough cylinders.
3. The boundary layer downstream of the stagnation point remains laminar in the presence of free stream turbulence and is forced into transition by surface roughness for the range of Reynolds number and turbulence levels tested.

4. Vorticity in the form of mean velocity gradients is amplified as it approaches the stagnation region.

5. Turbulent fluctuating velocity is amplified as it approaches the stagnation region, reaches a peak and then is damped as it approaches the boundary layer.

6. Heat transfer in the stagnation region is a maximum where turbulent fluctuations were found to be a minimum. This occurred between the wakes formed by parallel wires upstream and perpendicular to the axis of the cylinder. This corresponds to the region between vortex pairs where the velocity induced by the vortices was toward the cylinder surface. Conversely, the minimum heat transfer occurred where the induced velocity was away from the cylinder surface.

7. Vortices formed in the stagnation region from mean velocity gradients are well outside the theoretical laminar boundary layer.

REFERENCES

1. Frössling, N., "Evaporation, Heat Transfer, and Velocity Distribution in Two-Dimensional and Rotationally Symmetrical Laminar Boundary-Layer Flow," NACA TM-1432, 1958.

2. Smith, M.C., and Kuethe, A.M., "Effects of Turbulence on Laminar Skin Friction and Heat Transfer," Physics of Fluids, Vol. 9, No. 12, Dec. 1966, pp. 2337-2344.

3. Kestin, J., and Wood, R.T., "The Influence of Turbulence on Mass Transfer from Cylinders," Journal of Heat Transfer, Vol. 93, No. 11, Nov. 1971, pp. 321-327.

4. Giedt, W.H., "Effect of Turbulence Level of Incident Air Stream on Local Heat Transfer and Skin Friction on a Cylinder," Journal of the Aeronautical Sciences," Vol. 18, No. 11, Nov. 1951, pp. 725-730, 766.

5. Hanarp, L.R., and Sunden, B.A., "Structure of the Boundary Layers on a Circular Cylinder in the Presence of Free Stream Turbulence," Letters in Heat and Mass Transfer, Vol. 9, May-June 1982, pp. 169-177.

6. Lowery, G.W., and Vachon, R.I., "Effect of Turbulence on Heat Transfer from Heated Cylinders," International Journal of Heat and Mass Transfer, Vol. 18, No. 11, Nov. pp. 1229-1242.

7. Wang, C.R., "Turbulence and Surface Heat Transfer Near the Stagnation Point of a Circular Cylinder in Turbulent Flow," NASA TM-83732, 1984.

8. Gorla, R.S.R., and Nemeth, N., "Effects of Free Stream Turbulerce Intensity and Integral Length Scale on Heat Transfer From a Circular Cylinder in Crossflow," U. Grigull, et al., eds., Heat Transfer 1982, Vol. 3, Hemisphere Publishing Corp., Washington, D.C., 1982, pp. 153-158.

9. Sutera, S.P., Maeder, P.F., and Kestin, J., "On the Sensitivity of Heat Transfer in the Stagnation-Point Boundary Layer to Free-Stream Vorticity," Journal of Fluid Mechanics, Vol. 16, Part 4, Aug. 1963, pp. 497-520.

10. Sutera, S.P., "Vorticity Amplication in Stagnation-Point Flow and Its Effect on Heat Transfer, Journal of Fluid Mechanics, Vol. 21, Part 3, Mar. 1965, pp. 513-534.

11. Britter, R.E., Hunt, J.C.R., and Mumford, J. C., "The Distortion of Turbulence by a Circular Cylinder," Journal of Fluid Mechanics, Vol. 92, Part 2, May 28, 1979, pp. 269-301.

12. Sadeh, W.Z., and Brauer, H.J., "Coherent Substructure of Turbulence Near the Stagnation Zone of a Bluff Body," Journal of Wind Engineering and Industrial Aerodynamics, Vol. 8, No. 1-2, July 1981, pp. 59-72.

13. Sadeh, W.Z., and Sullivan, P.P., "Turbulence Amplification in Flow About an Airfoil," ASME Paper 80-GT-111, Mar. 1980.

14. Hodson, P.R., and Nagib, H.M., "Vortices Induced in a Stagnation Region by Wakes-Their Incipient Formation and Effects on Heat Transfer from Cylinders," AIAA Paper 77-750, June 1977.

15. Morkovin, M.V., "On the Question of Instabilities Upstream of Cylindrical Bodies," NASA CR-3231, 1979.

16. Schlichting, H., "Boundary Layer Theory," 4th ed., McGraw Hill, p. 78.

17. Jansen, B.J. Jr., "Flow Visualization Through the Use of the Smoke Wire Technique," AIAA Paper 81-0412, Jan. 1981.

18. Hippensteele, S.A., Russell, L.M., and Stepka, F.S., "Evaluation of a Method for Heat Transfer Measurements and Thermal Visualization Using a Composite of a Heater Element and Liquid Crystals," Journal of Heat Transfer, Vol. 105, No. 1, Feb 1983, pp. 184-189.

19. VanFossen, G.J., et al, "Heat Transfer Distributions Around Nominal Ice Accretion Shapes Formed on a Cylinder in the NASA Lewis Icing Research Tunnel," AIAA Paper 84-0017, Jan. 1984.

20. Kline, S.J., and McClintock, F.A., "Describing Uncertainties in Single-Sample Experiments," Mechanical Engineering, Vol. 75, No. 1, Jan. 1953, pp. 3-8.

21. Marziale, M.L., and Mayle, R.E., "Mass Transfer From a Circular Cylinder-Effects of Flow Unsteadiness and 'Slight Nonuniformities';" Rensselaer Polytechnic Institute, Troy, New York, Sept. 1984. (NASA CR-174759).

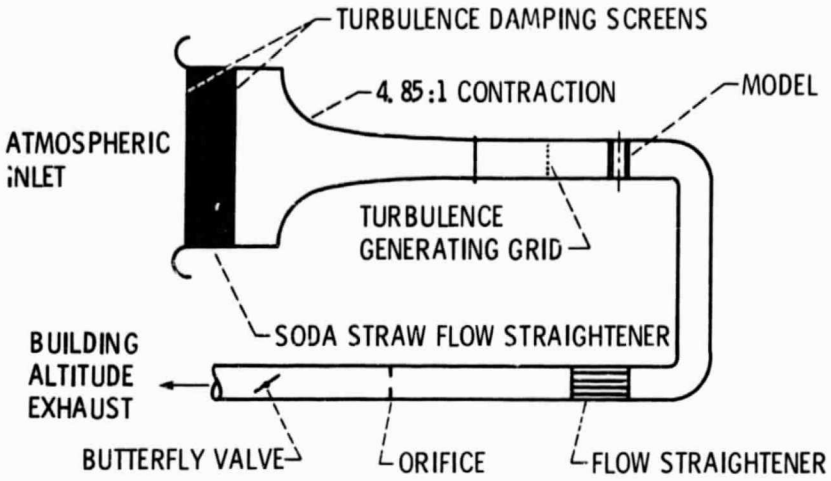

Figure 1. - Schematic of wind tunnel.

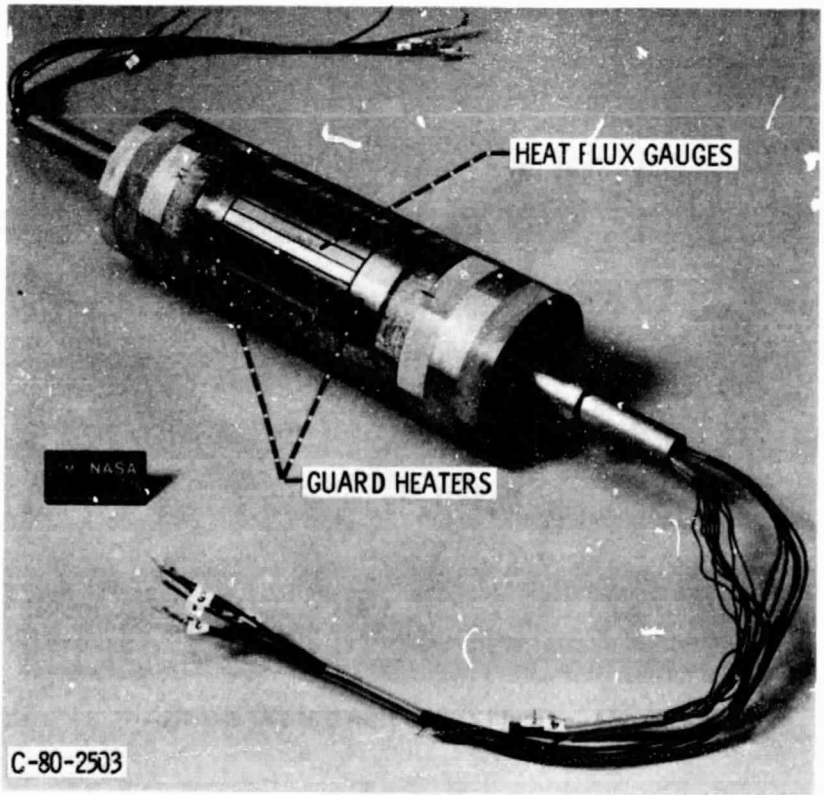

Figure 2. - Spanwise average heat transfer model.

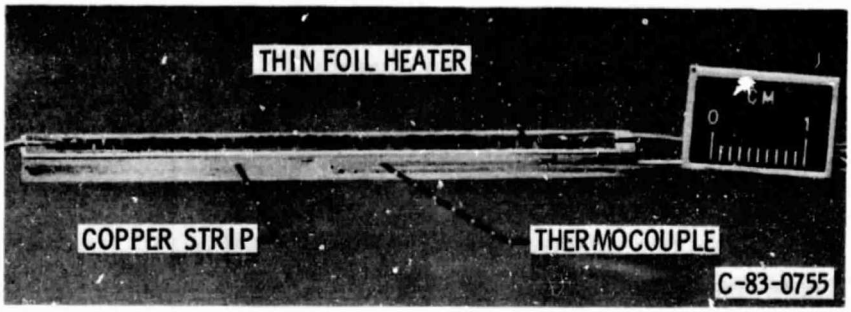

Figure 3. - Photograph of heat flux guage.

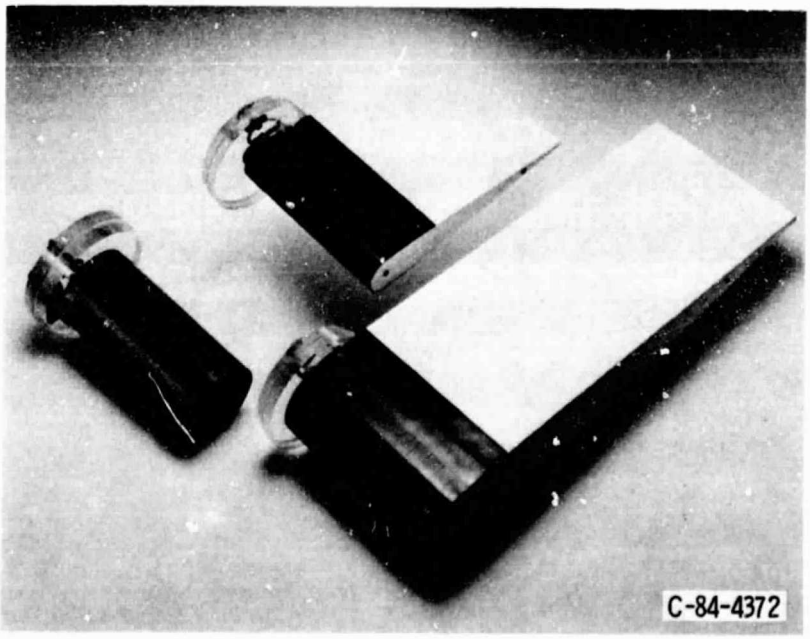

Figure 4. - Liquid crystal heat transfer models.

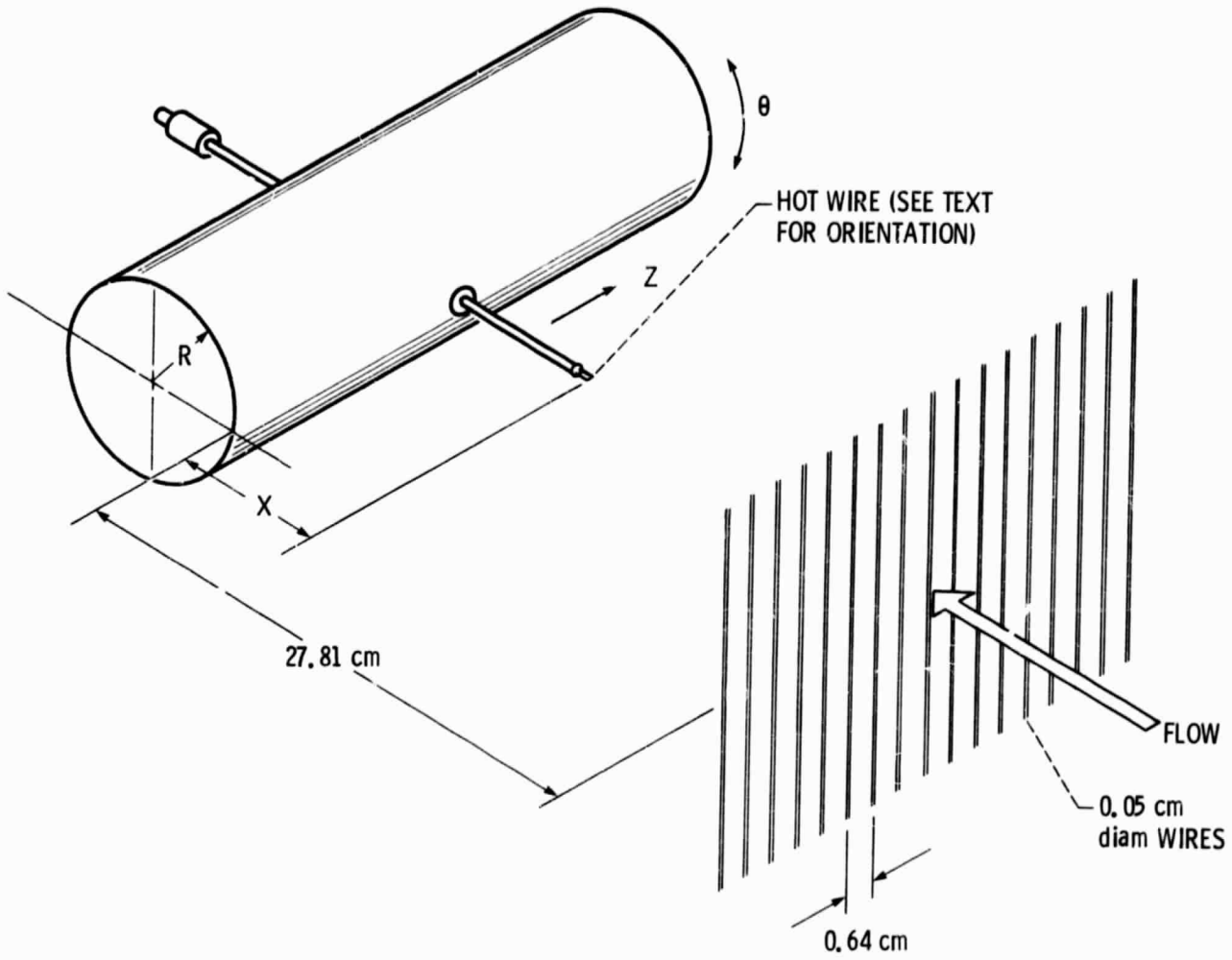

Figure 5. - Traversing cylinder and upstream array of wires.

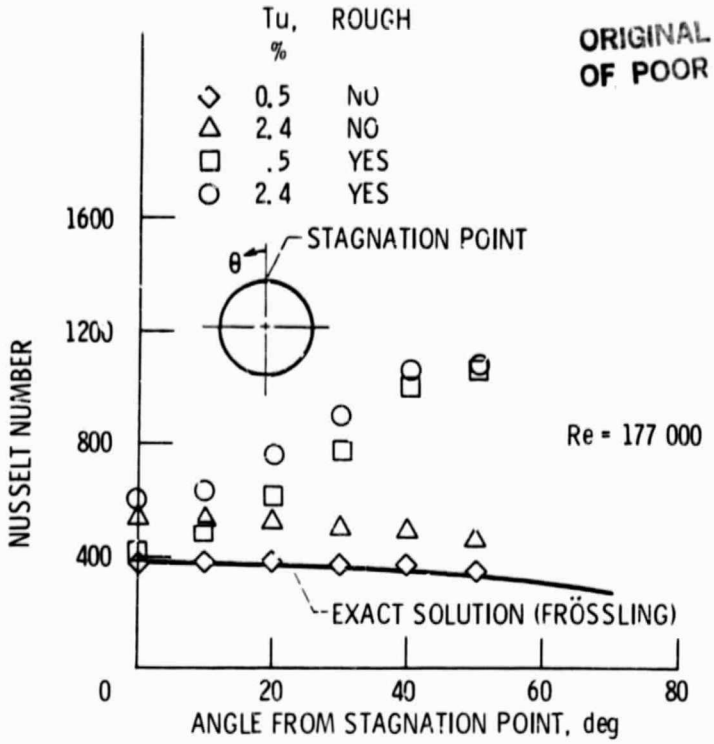

Figure 6. - The effect of free-stream turbulence and surface roughness on spanwise averaged heat transfer for a cylinder in crossflow.

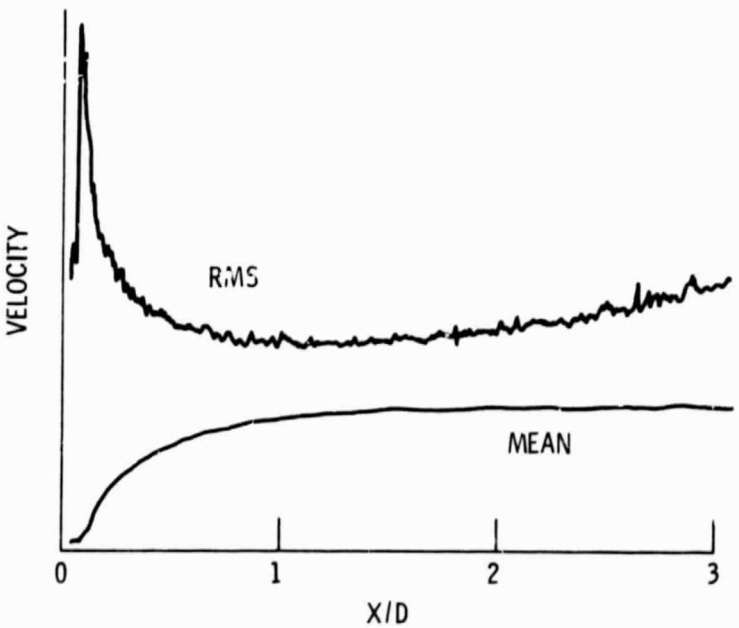

Figure 7. - Streamwise traverse of a hot wire close to the stagnation streamline.

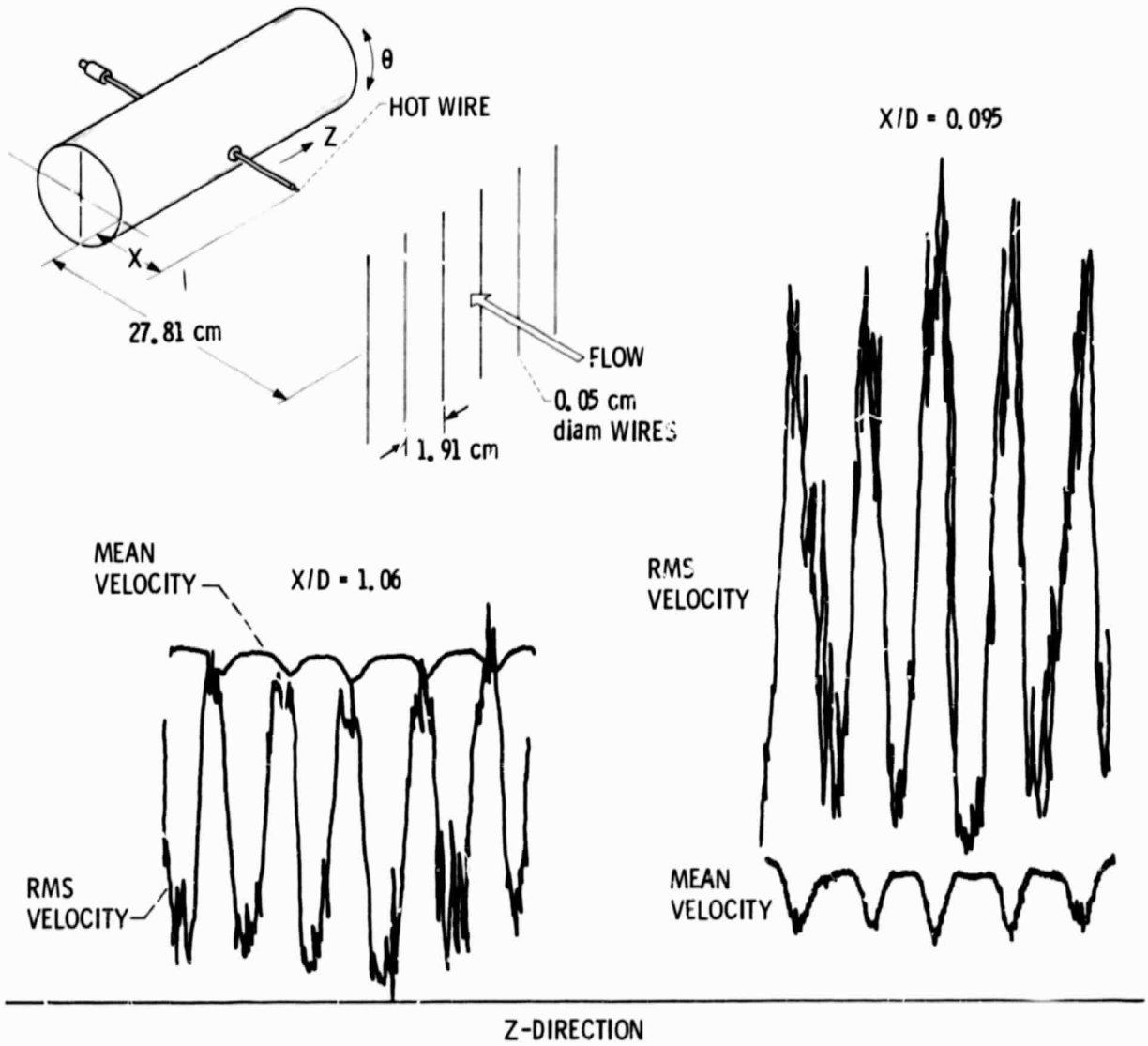

Figure 8. - Spanwise traverses of a hot wire near the cylinder stagnation point. (NOTE: Abscissa of RMS and mean velocity plots offset slightly due to pen offset on x-yy' recorder.)

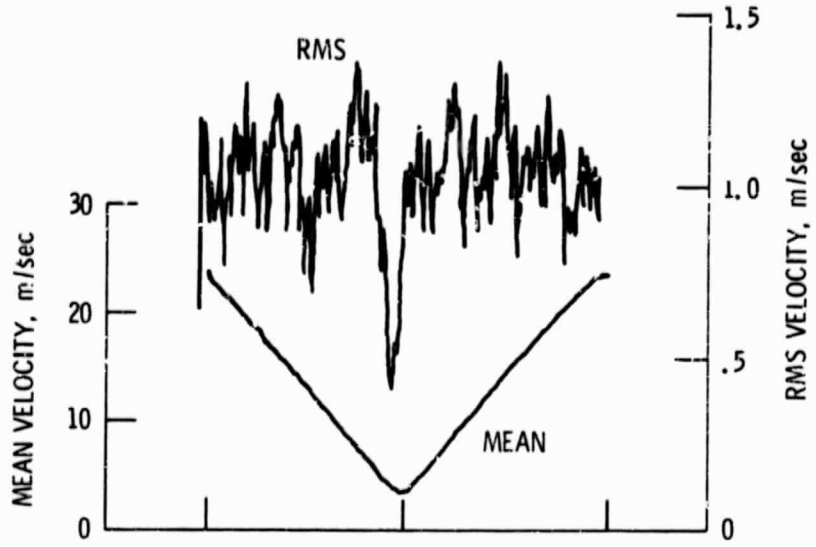

(a) Clear tunnel.

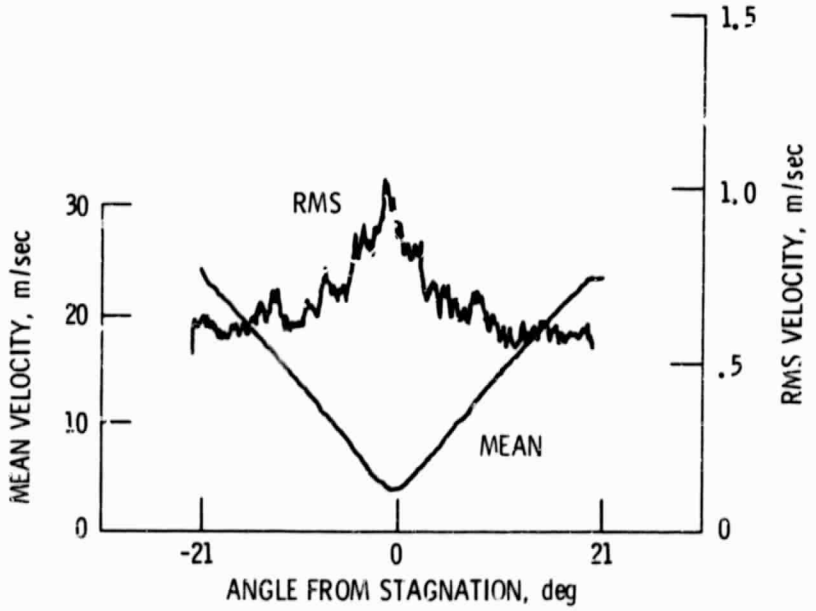

(b) Wire array upstream.

Figure 9. - θ-direction hot wire traverse. Re_D = 125 000.

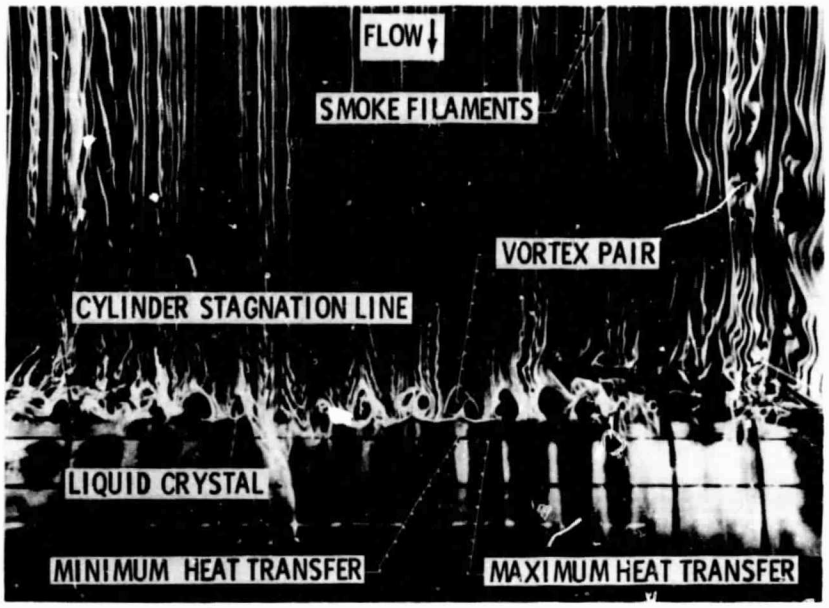

Figure 10. - Combined thermal and flow visualization of cylinder in cross flow.

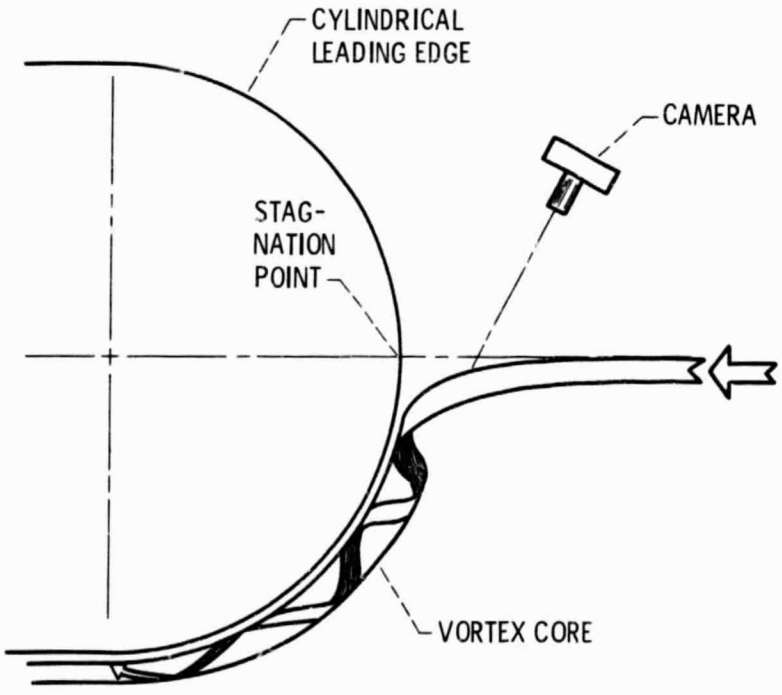

Figure 11. - Liquid crystal model and relative camera position.

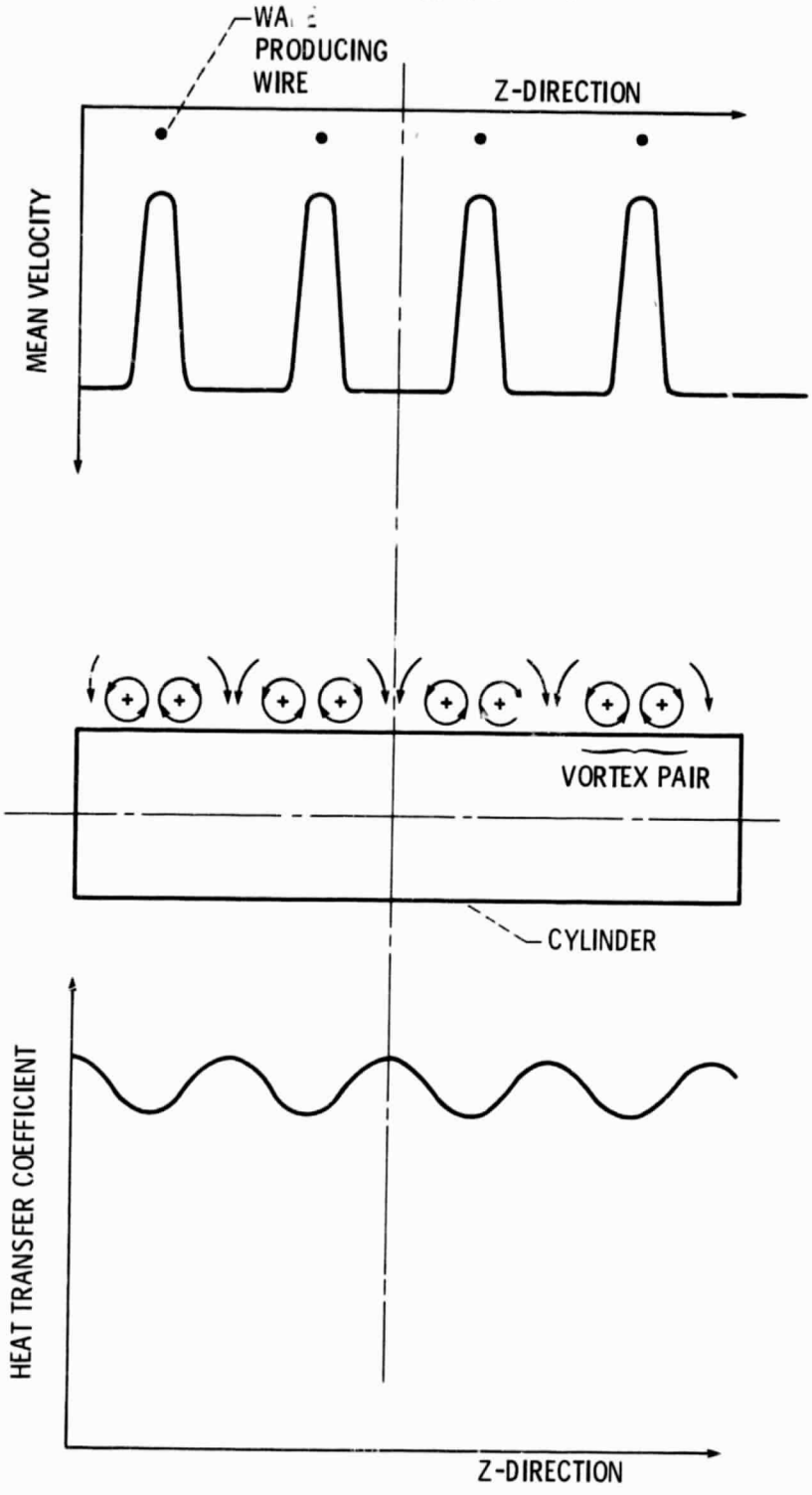

Figure 12. - Schematic showing relationship of wire produced wakes, vortex pairs and peaks in heat transfer.